Available online at www.sciencedirect.com
SCIENCE DIRECT
Catalysis Today 105 (2005) 507–515
CATALYSIS TODAY
www.elsevier.com/locate/cattod

Formation of textural and mechanical properties of extruded ceramic honeycomb monoliths: An ^{1}H NMR imaging study

S.A. Yashnik [a], Z.R. Ismagilov [a,*], I.V. Koptyug [b], I.P. Andrievskaya [a], A.A. Matveev [b], J.A. Moulijn [c]

[a] *Boreskov Institute of Catalysis, Novosibirsk, 630090, Russia*
[b] *International Tomography Center, Novosibirsk, Russia*
[c] *Technical University of Delft, The Netherlands*

Abstract

The effects of the nature of oxide component and binder, and thermal treatment temperature (100 °C and from 600 to 1300 °C) on textural and physicochemical properties of honeycomb monoliths based on alumina, titania and aluminosilicates have been studied.

The main regularities of the texture formation have been revealed using ^{1}H NMR imaging, SEM, XRD, adsorption technique and others. It has been shown that the textural changes of monolith samples at different preparation stages from extrusion to thermal treatment are mostly caused by removal of capillary water (20–100 °C), sintering of small pores and consolidation of oxide particles (100–700 °C), and phase transformation of the oxide component or the binder (900–1300 °C).

Keywords: Honeycomb monolith catalyst; ^{1}H NMR imaging; Extrusion; Texture; Pore structure; Mechanical strength

1. Introduction

Today monolith supports with honeycomb structure and catalysts on their basis are widely used in various branches of industry [1–4]. Most actively monolithic catalysts are applied for purification of automobile exhaust gases [1,5] and waste gases of chemical, metallurgical and energy producing plants [2,3] from pollutants, such as hydrocarbons, carbon monoxide, nitrogen oxides, hydrogen sulfide, volatile organic compounds, etc. The development of monolithic catalysts increases their technical merit due to ease of operation and regeneration owing to low pressure drop, small dust and attrition sensitivity [1,2,5].

Extrusion on vacuum presses is the most widely used method for preparation of honeycomb monolithic supports. The production of honeycomb monolithic substrate includes the following technological stages: preparation of the forming mass, its extrusion through a die, dry-curing, drying and thermal treatment [5].

The rational compositions of the extrusion mass containing the main oxide component, the binder and the plasticizer are selected to provide both optimum rheological properties of the mass and optimum physicochemical properties of the final monolithic substrate. Various oxide powders, such as titania, zirconia, silica and alumina [2], mullite, spodumene, cordierite [1,2,5], kaolin, montmorillonite, halloysite clays [2] and their compositions, are widely used. A binder and a plasticizer varying in concentration and preparation method are added to the forming mass to give them plasticity [1,5,6]. Clays from different deposits, kaolin, montmorillonite, and the product of thermal dispersion of alumina hydrate are usually used as the binder.

The thermal treatment is the final stage in the production of honeycomb monoliths, which determines their operational properties [1,2], such as mechanical strength, specific

* Corresponding author. Tel.: +7 3833 306219; fax: +7 3833 397352.
E-mail address: zri@catalysis.nsk.su (Z.R. Ismagilov).

0920-5861/$ – see front matter © 2005 Published by Elsevier B.V.
doi:10.1016/j.cattod.2005.06.055

surface area and pore structure. Chemical and phase transformations and sintering processes forming the support texture and physicochemical properties can take place during the thermal treatment of ceramic supports. Therefore, it is important to have detailed information on the formation of the above properties at each technological stage.

In the current study, the formation of the textural and physicochemical properties of ceramic monoliths based on alumina, titania and aluminosilicates has been investigated by ^{1}H NMR microimaging in combination with a number of traditionally used methods (XRD, SEM, mercury porosimetry and others) during dry-curing, drying and thermal treatment. The non-destructive character of the ^{1}H NMR microimaging method is attractive because it makes possible visualization of the dynamics of the substrate texture formation at various preparation stages, which is important for optimization of the technology for synthesis of substrate with desired operational characteristics.

2. Experimental

2.1. Preparation of monoliths

The masses for extrusion were composed by mixing Al_2O_3, TiO_2 or clay powders with aluminum hydroxide sol having pseudoboehmite structure or Ca-form of montmorillonite (Tagan deposit) in a Z-shape mixer. The water content of the extrusion masses was 33–35%. The masses had the following compositions (calculated for the dry products):

- alumina: γ-Al_2O_3 (60 wt.%), α-Al_2O_3 (10 wt.%) and γ-Al_2O_3 or Ca-montmorillonite (30 wt.%);
- titania: anatase (60 wt.%), rutile (10 wt.%) and Ca-montmorillonite (30 wt.%);
- aluminosilicate: clay (75 wt.%) and Ca-montmorillonite (25 wt.%).

Honeycomb monoliths were extruded using a pneumatic press with a vertical piston and dies with diameter of 11 and 21 mm. The extruded monoliths were dry-cured for 2–5 days, dried at 100 °C for 4–8 h and calcined at desired temperatures (600–1300 °C) for 4 h.

Depending on the composition and the calcination temperature, the wall thickness was 0.3–0.5 mm, the channel density was 169–225 cpsi and 100–135 cpsi for monoliths extruded using 11 and 21 mm dies, respectively.

2.2. ^{1}H NMR microimaging technique

^{1}H NMR imaging experiments were performed using a Bruker "Avance-300" NMR spectrometer equipped with a microimaging accessory capable of delivering gradient pulses of up 100 G/cm. Experimental details can be found elsewhere [7].

2.3. Determination of monolith shrinkage

The shrinkage of monoliths along the diameter and length was determined after dry-curing, drying and thermal treatment of the samples relative to their "raw" state right after extrusion:

- Along the diameter: $S_d = (D_0 - D_t)/D_0 \times 100\%$, where D_0 and D_t are monolith diameters after extrusion and thermal treatment, respectively.
- Along the length: $S_l = (L_0 - L_t)/L_0 \times 100\%$, where L_0 and L_t are monolith lengths after extrusion and thermal treatment, respectively.

2.4. Physicochemical methods

XRD analysis of the samples was carried out using a HZG-4C (Freiberger Prazisionmechanik) diffractrometer with monochromatic Cu Kα irradiation. The phase compositions were determined using diffraction patterns recorded in the 2θ range 4–40° with 1°/min scanning rate.

Specific surface area (S, m^2/g) of the samples was determined using thermal desorption of argon. Total pore volume (V_Σ, cm^3/g) was determined by mercury porosimetry in the effective pore radius (R_{ef}) range from 4 to 10^5 nm using a Porosiger-9300 instrument. True density (ρ, g/cm^3) of the samples was measured using a helium Autopicnometer-1320.

Porosity was calculated as follows: $\varepsilon = V_\Sigma/(V_\Sigma + 1/\rho) \times 100\%$, where ε is the sample porosity, %, V_Σ is the total pore volume according to the mercury porosimetry data, cm^3/g, and ρ is the true density of the sample, g/cm^3.

Crushing mechanical strength was determined using an MP-9C instrument. The method is based on the measurement of the force required for crushing of a monolith between two parallel plates. Mechanical strength of the sample along the generatrices was calculated using the following formula: $P_g = p/S = p/(d \times L)$, where P_g is the sample strength, kg/cm^2, p is the value on the instrument indicator, kg, S is the cross-section area of the monolith, cm^2, d is the "effective" sample diameter, cm, L is the sample height, cm. The "effective" sample diameter was accepted to be equal to the monolith diameter (D_t) minus the size of the sum of internal opening (channels).

The physicochemical properties of honeycomb monoliths based on alumina, titania and aluminosilicate are presented in Tables 1–4.

The support morphology was studied using a REM 100-U scanning electron microscope. The accelerating voltage was 20 kV.

3. Results and discussion

The most important properties of air-dry ceramic supports, such as pore structure, specific surface area,

Table 1
Physicochemical properties of alumina monolith with pseudoboehmite as binder

$T_{calc.}$ (°C)	XRD composition	S (m^2/g)	ρ (g/cm^3)	Total pore volume, V_Σ (cm^3/g) and R_{ef} (Å)	True porosity ε (%)	Mechanical strength, P_g, (kg/cm^2)	Shrinkage, S_d (%)/S_l (%)
100	Pseudoboehmite γ-Al_2O_3 α-Al_2O_3	140	–	$V_\Sigma = 0.38$ $R_{ef} = 70$	–	–	4/3.5
600	γ-Al_2O_3 α-Al_2O_3 (trace)	156	–	$V_\Sigma = 0.37$ $R_{ef} = 72$	–	17	5/4.5
800	γ-Al_2O_3 α-Al_2O_3 (trace)	115	–	–	–	17.5	–
900	θ-Al_2O_3 (70%) α-Al_2O_3 (30%)	95	–	$V_\Sigma = 0.41$ $R_{ef} = 110$	–	9.0	7/6
1000	θ-Al_2O_3 (50%) α-Al_2O_3 (50%)	50	3.762	$V_\Sigma = 0.36$ $R_{ef} = 160$	59	21	–
1100	θ-Al_2O_3 (40%) α-Al_2O_3 (60%)	25	–	$V_\Sigma = 0.33$ $R_{ef} = 240$	–	17	–
1200	α-Al_2O_3	9	4.043	$V_\Sigma = 0.26$ $R_{ef} = 735$	54	37	17/15.5
1300	α-Al_2O_3	7	3.902	$V_\Sigma = 0.24$ $R_{ef} = 1290$	48	52	20/18.5

Mass composition, wt.%: 60% γ-Al_2O_3 + 10% α-Al_2O_3 + 30% pseudoboehmite, Fe content < 0.05 wt.%.

Table 2
Physicochemical properties of alumina monolith with Ca-montmorillonite as binder

$T_{calc.}$ (°C)	XRD composition	S (m^2/g)	Total pore volume V_Σ (cm^3/g) and R_{ef}, (Å)	Mechanical strength, P_g (kg/cm^2)	Shrinkage, S_d (%)/S_l (%)
100	Ca-montmorillonite γ-Al_2O_3 α-Al_2O_3	150	$V_\Sigma = 0.34$ $R_{ef} = 72$	–	8.5/8
600	γ-Al_2O_3 α-Al_2O_3 (trace) $Ca_{0.2}(Al, Mg)_2Si_4O_{10}(OH)_2$*$4H_2O$ α-SiO_2 (trace)	146	$V_\Sigma = 0.34$ $R_{ef} = 76$	32	9/8.5
900	γ*-Al_2O_3 α-Al_2O_3 (trace) α-SiO_2 (trace) amorphous SiO_2 (trace) $Al_6Si_2O_{13}$ (trace, mullite)	81	$V_\Sigma = 0.34$ $R_{ef} = 95$	43	10/9
1100	α-Al_2O_3 δ-Al_2O_3 (trace) SiO_2 and α-SiO_2 $Al_6Si_2O_{13}$ (mullite) $MgSiO_3$	33	$V_\Sigma = 0.33$ $R_{ef} = 210$	39	11.5/10
1200	α-Al_2O_3 (main) SiO_2 (main) and α-SiO_2 $Al_6Si_2O_{13}$ (mullite) $MgSiO_3$ (trace)	7	$V_\Sigma = 0.32$ $R_{ef} = 540$	42	12/11
1300	α-Al_2O_3 (main) SiO_2 (main) and α-SiO_2 $Al_6Si_2O_{13}$ (mullite) $MgSiO_3$ (trace)	6	$V_\Sigma = 0.29$ $R_{ef} = 1170$	60	14/12

Mass composition (wt.%): 60% γ-Al_2O_3 + 10% α-Al_2O_3 + 30% Ca-montmorillonite, Fe content ~0.3 to 0.4 wt.%.

Table 3
Physicochemical properties of titania monolith with Ca-montmorillone

$T_{calc.}$ (°C)	XRD composition	S (m^2/g)	ρ (g/cm^3)	Total pore volume, V_Σ (cm^3/g) and R_{ef} (Å)	True porosity ε (%)	Mechanical strength, P_g (kg/cm^2)	Shrinkage, S_d (%)/S_l (%)
100	Anatase (70 Å) Rutile (trace) Montmorillonite α-SiO_2 (trace)	185	–	V_Σ = 0.44	–	–	12/8.5
700	Anatase (300 Å) Rutile (trace) Montmorillonite α-SiO_2 (trace)	72	–	V_Σ = 0.41 R_{ef} = 160	–	17	13/9.5
800	Anatase (400 Å) Rutile Amorphous SiO_2 α-SiO_2 (trace)	20	–	V_Σ = 0.26 R_{ef} = 265	–	23	–
900	Anatase (400 Å) Rutile (500 Å, 10%) Amorphous SiO_2 α-SiO_2	16	3.258	V_Σ = 0.08 R_{ef} = 400	19.8	63	30/27
1200	Putile (1000 Å) $Al_6Si_2O_{13}$ (mullite) $MgSiO_3$ α-SiO_2 (trace)	0.01	3.073	V_Σ = 0.11 R_{ef} = 9180	25.0	66	30/27
1300	Putile (>1000 Å) $Al_6Si_2O_{13}$ (mullite) $Mg_2Al_4Si_5O_{18}$ α-SiO_2 (trace)	0.01	3.115	V_Σ = 0.23 R_{ef} = 27400	42.0	74	18/22

Mass composition (wt.%): 60% anatase + 10% putile + 30% Ca-montmorillonite; Fe content ~0.3 to 0.4 wt.%.

texture, mechanical strength, density, water resistance, etc., are known to be formed during their thermal treatment [3]. The results of the investigation of physicochemical properties of monolith supports on the basis of alumina, titania and aluminosilicate dried at 100 °C and calcined at temperatures from 600 (700) to 1100–1300 °C indicate that independent of the type of the oxide an increase of the calcination temperature results in changes of the monolith geometric sizes (diameter, length, channel density), decrease of the total pore volume and specific surface area, which generally lead to an increase of the ceramic support mechanical strength (Tables 1–4).

Table 4
Physicochemical properties of aluminosilicate monolith with Ca-montmorillonite as binder

$T_{calc.}$ (°C)	XRD composition	S (m^2/g)	ρ (g/cm^3)	Total pore volume, V_Σ (cm^3/g) and R_{ef} (Å)	True porosity, ε (%)	Mechanical strength, P_g (kg/cm^2)	Shrinkage, S_d (%)/S_l (%)
100	α-SiO_2 Kaolin Montmorillonite (trace)	59	–	V_Σ = 0.12	–	–	8.5/7.5
700	α-SiO_2 Montmorillonite (amorphous)	37	–	V_Σ = 0.12 R_{ef} = 300	–	22	9/8
800	α-SiO_2 Amorphous SiO_2	0.8	-	V_Σ = 0.18 R_{ef} = 8850	–	31	–
900	α-SiO_2 Amorphous SiO_2	0.4	2.584	V_Σ = 0.11 R_{ef} = 9220	22	39	10.5/10
1000	α-SiO_2 SiO_2 $Al_6Si_2O_{13}$ (mullite)	0.3	2.631	V_Σ = 0.18 R_{ef} = 18975	32	47	10.5/10
1100	α-SiO_2 $Al_6Si_2O_{13}$ (mullite) $MgSiO_3$	0.3	2.495	V_Σ = 0.14 R_{ef} = 14960	26	49	10.5/10

Mass composition (wt.%): 75% clay + 25% Ca-montmorillonite, Fe content ~1.6 to 1.8 wt.%.

3.1. Alumina honeycomb monoliths

The effects of the dry-curing (25 °C, 0–72 h) and thermal treatment conditions on the formation of the pore structure of alumina monoliths have been studied by ^{1}H NMR imaging method.

Fig. 1 presents two-dimensional images of the water content in alumina monoliths as a function of the dry-curing time. One can see that the ^{1}H NMR signal intensity goes down during the dry-curing. The maximum (3-fold) decrease of the ^{1}H NMR signal was observed during the first 24 h of dry-curing (Fig. 2). The ^{1}H NMR imaging data are in a good agreement with the data on the drying loss in the sample at 110 °C determined by thermal gravimetric analysis. The value of drying loss for the ''raw'' sample found to be 30 wt.% and goes down to 10 wt.% after dry-curing for 24 h and to 3 wt.% in the following 48 h of dry-curing.

During the experiments it has been shown that the samples subjected to dry-curing of different duration are characterized by different relaxation times T_1 and T_2. During the first 24 h of dry-curing the T_1 and T_2 values decrease most significantly (more than 4-fold, Fig. 2). On the base of ^{1}H NMR imaging fundamentals, we conclude that water molecules are rather free in the pore structure of the ''raw'' monolith at high water content, but during dry-curing most of ''free'' water is removed and remaining molecules are bonded to the walls of pores stronger than molecular to molecular binding in free water [8].

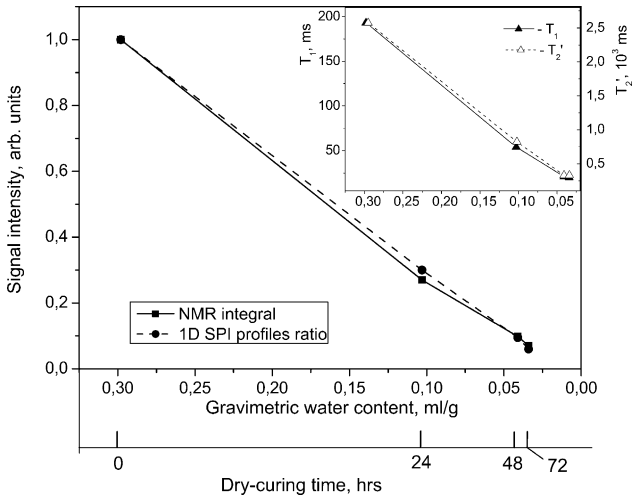

Fig. 2. Correlation of the ^{1}H NMR signal intensity with the gravimetric water content in the alumina monolith during the dry-curing procedure.

The maximum drying loss during the sample dry-curing is accompanied by a decrease of its geometric dimensions (diameter and length, Table 1). The sample shrinkage during the first 24 h is about 4%. It should be noted that shrinkage of the alumina monoliths with the temperature growth from 100 to 900 °C is ~6.5% and sharply increases up to 17% after calcination at 1200 °C.

The pore structure of air-dry samples (100 °C) is biporous according to the mercury porosimetry data (Fig. 3). It is composed of small pores with the radii ~45 to 50 Å and

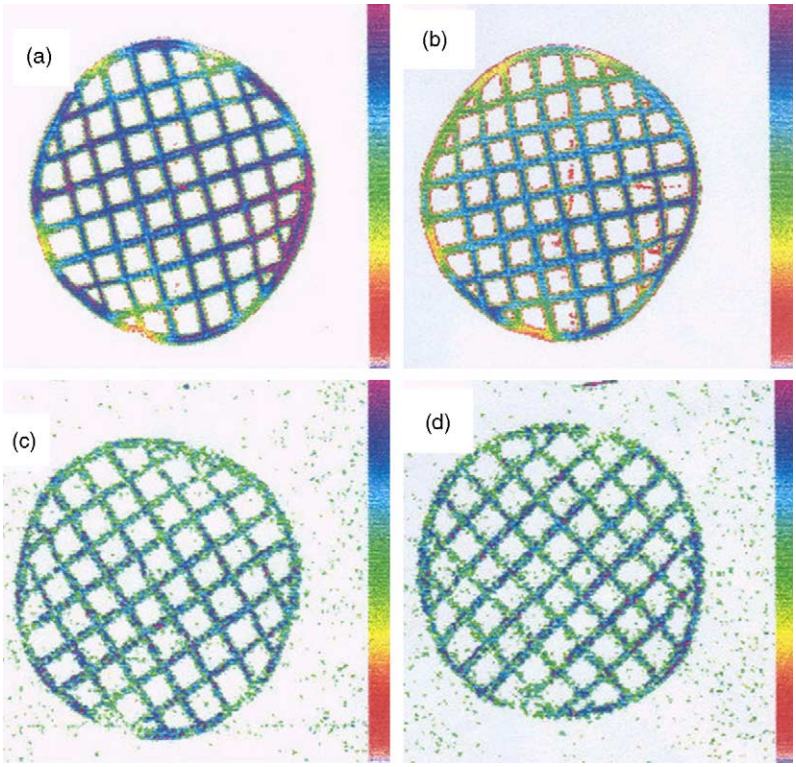

Fig. 1. Two-dimensional ^{1}H NMR images of water content in a alumina monolith depending on dry-curing time: (a) 0 h; (b) 24 h; (c) 48 h; and (d) 72 h.

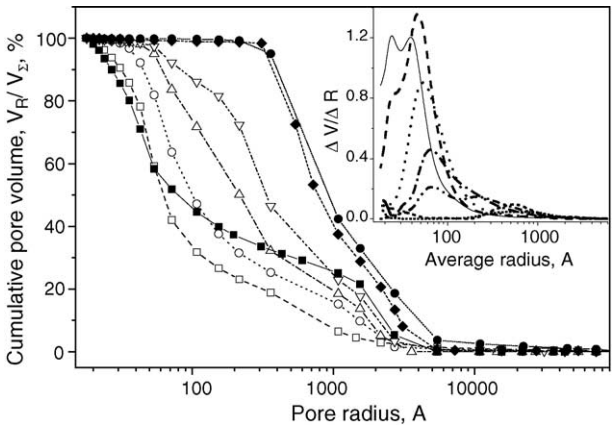

Fig. 3. Cumulative pore volume as V_R/V_Σ in % (a) and derivative pore volume (b) curves for alumina monoliths calcined at 100 (■, $V_\Sigma = 0.38\ cm^3/g$); 600 (□, $V_\Sigma = 0.36\ cm^3/g$); 900 (○, $V_\Sigma = 0.41\ cm^3/g$); 1000 (△, $V_\Sigma = 0.36\ cm^3/g$); 1100 (▽, $V_\Sigma = 0.33\ cm^3/g$); 1200 (◆, $V_\Sigma = 0.25\ cm^3/g$); and 1300 °C (●, $V_\Sigma = 0.23\ cm^3/g$).

large pores with the radii 200–1500 Å. For alumina samples, an increase of the calcination temperature is accompanied by changes of textural characteristics. Calcination at 600 °C leads to the increase of the fraction of small pores (from 50 to 60%) and growth of their average radius to 75–80 Å. Meanwhile, the fraction of pores with the 200–1500 Å radii slightly decreases. According to the mercury porosimetry data, further increase of the calcination temperature from 600 to 1300 °C leads to the pore volume decrease from 0.44 to 0.24 cm^3/g accompanied by an increase of the predominating pore radius from 75–80 to 700–1000 Å. At calcination temperatures above 900 °C, the sharpest decrease is observed for volume of pores with the radii smaller than 100–200 Å. Pores with the radii of 100–200 Å are absent in the samples calcined at 1200–1300 °C, whereas the fraction of pores with the radii smaller than 400 Å does not exceed 5–8%. Meanwhile, the volume fraction of pores with the radii of 500–5000 Å significantly increases (to ~90%).

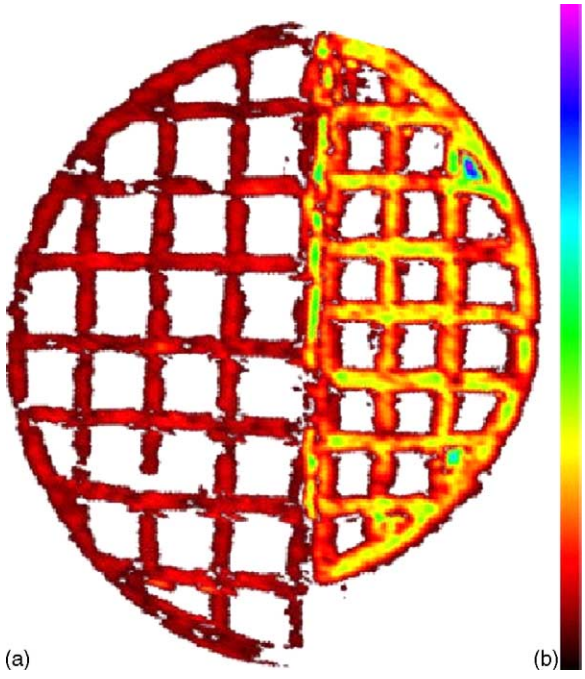

Fig. 4. ^{1}H NMR images of two alumina half monolith samples calcined at 600 °C (a) and 1200 °C (b) after their saturation with water.

^{1}H NMR imaging method made it possible to visualize the differences in the pore structure of alumina monoliths formed after calcination at different temperatures. Fig. 4 presents two-dimensional maps of water content in two adjacent halves of alumina monoliths calcined at temperatures 600 °C and 1200 °C, the pore space of which was initially filled with water. One can see that the ^{1}H NMR signal intensity in the monolith half calcined at 1200 °C is higher (yellow and orange colors) than in the monolith half calcined at 600 °C (vinous color) whereas the pore volume is almost two times lower. This phenomenon may be explained by different radii of predominating pores. The relaxation times of adsorbed liquid are known to be usually short in small pores (for example, in zeolite crystallites [9]). As a result, ^{1}H NMR signal corresponding to the water content in the zeolite channels may not be observed in the experiments. In the sample calcined at 1200 °C the major fraction of the pore space consists of large pores with the radii of 500–3000 Å where water practically does not experience the effect of the monolith walls (free water). Meanwhile, small pores with the radii ~45 to 80 Å predominate in the sample calcined at 600 °C. This results in a decrease of the relaxation times and ^{1}H NMR signal intensity.

The textural changes of alumina monoliths were regularly accompanied by changes of the other physicochemical properties (Fig. 5). In the calcination temperature range 600–900 °C the specific surface area, pore volume, porosity and mechanical strength of the samples changed smoothly. A sharp decrease of the surface area and total pore volume, and significant increase of the mechanical strength were observed at higher calcination temperatures (1000–

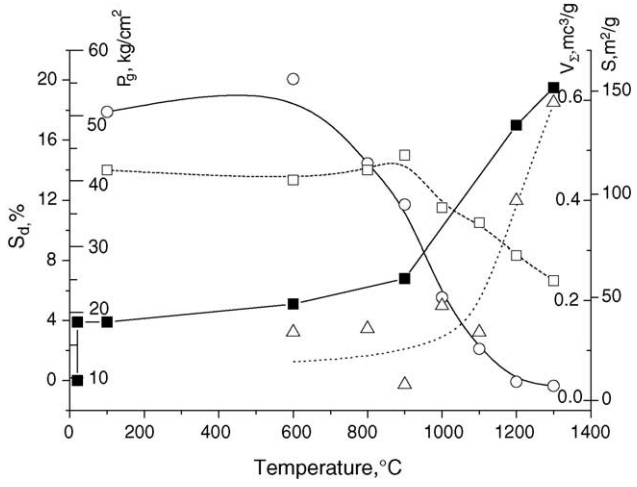

Fig. 5. Changes in the surface area, S, m^2/g (○); pore volume, V_Σ, cm^3/g (□); shrinkage, S_d, % (■); and mechanical strength, P_g, kg/cm^2 (△) of the alumina monolith depending on calcination temperature.

1300 °C). For instance, specific surface area of samples calcined at 600 and 1300 °C was 156 and 7 m^2/g, respectively (Table 1). The sample porosity went down from 60 to 48%. Meanwhile, the mechanical strength grew from 17 to 52 kg/cm^2 (Table 1).

Changes of the geometrical parameters of the monoliths correlate with the changes of the pore volume (Fig. 5). This fact makes it possible to suggest that shrinkage of alumina monoliths is primarily caused by changes of their pore space. The pore structure formation of monoliths prepared by extrusion of a well-milled oxide material with a binder may be split into several stages. During preparation of the extrusion mass the binder is uniformly distributed between the solid oxide particles. In this case, aluminum hydroxide sol is distributed between the particles of γ-Al_2O_3 powder. Intensive mixing results in thixotropic peptization of the binder, and the mass acquires connectedness, plasticity and, consequently, formability.

The pore structure of the samples at dry-curing and drying stages is determined by two factors acting in opposite directions: the value of capillary forces compressing the structure and the degree of its resistibility to compression. The first factor depends on the paste humidity before forming, mechanical densification of the mass in the mixing device and surface tension of the intermicellar liquid [10]. The second factor is determined by the particle size and strength of primary crystallites inside a particle [10]. During drying, hydroxyl groups of aluminum hydroxide sol and solid γ-Al_2O_3 particles condense to form colloid bridges, which accounts for the formation of strong bonds and results in the structure contraction. This contraction leads to a decrease of the capillary radii and, consequently, an increase of the water connectedness in them, which is observed by ^{1}H NMR imaging as a decrease of relaxation times T_1 and T_2 in the samples during dry-curing.

The pore structure of the samples during thermal treatment at different temperatures (600–1300 °C) is determined by sintering of the pores and phase transformations. The following conclusions were made on the basis of pore size distributions measured by mercury porosimetry and data on the particle sizes observed by SEM. Changes of the pore structure and specific surface area in the temperature range of 600–900 °C are mostly caused by sintering of small pores and consolidation of alumina particles, that was earlier observed for granulated alumina [10–12]. The sintering of small pores results in a slight decrease of the total pore volume and has practically no effect on the geometrical sizes of the samples. On the contrary, a sharp decrease of the total pore volume observed after calcination at 1000–1300 °C leads to a significant decrease of the geometrical dimensions of the samples. Changes of the pore structure in the temperature range of 1000–1300 °C are caused by reconstruction of alumina structure, which ends at 1200 °C with the formation of α-Al_2O_3. According to the XRD data (Table 1), alumina samples calcined at 600 °C contained ∼90% γ-Al_2O_3 and ∼10% α-Al_2O_3 introduced into the extrusion mass. The appearance of additional α-Al_2O_3 was observed at 900 °C (∼30% α-Al_2O_3 and ∼70% θ-Al_2O_3), and its concentration increased to 100% after calcination at 1200 °C.

So, changes of the geometric dimensions of alumina monoliths may be tentatively split into three temperature regions. In the temperature range of 20–100 °C, i.e. during dry-curing and drying of the samples, the sample shrinkage takes place due to removal of the capillary water from the alumina pore space. During calcination of the sample at 600–900 °C changes of the geometrical parameters of the monoliths are related to changes of their textural properties, namely, pore volume and radius. The shrinkage observed after calcination of the samples at temperatures above 900 °C is caused by the reconstruction of the γ-Al_2O_3 structure, which ends at 1200 °C with the formation of α-Al_2O_3.

The formation of the pore structure of monoliths prepared by extrusion is also affected by the nature of the binder and changes of its texture at different technological stages. The use of Ca-montmorillonite instead of aluminum hydroxide sol as a binder results in a more significant change of the geometrical dimensions of alumina monoliths at the dry-curing stage. For extrusion masses of the same composition, the monolith shrinkage along the diameter at the dry-curing stage was 4 and 9% for samples prepared using aluminum hydroxide sol and Ca-montmorillonite, respectively (Tables 1 and 2). Montmorillonite has a layered structure, and its swelling in water is due to introduction of water molecules into the layers of the silica framework and corresponding increase of the interlayer spacing. The water removal during dry-curing leads to a decrease of the interlayer spacing, appearance of three-dimensional strains in the material, and, correspondingly, strong contraction of the product pore space. After calcination in the temperature range of 600–1200 °C changes of the pore volume, and, consequently, geometrical size of alumina monoliths prepared using aluminum hydroxide sol and montmorillonite were close to each other (Tables 1 and 2), being caused by similar processes.

3.2. Titania honeycomb monoliths

An investigation of the texture formation of honeycomb monoliths on the basis of titania by ^{1}H NMR imaging is restricted because the presence of paramagnetic Fe^{3+} (∼0.4 wt.%) ions leads to a decrease of the water spin relaxation time T_1 and T_2. The latter causes poor resolution of ^{1}H NMR imaging. For titania monoliths calcined at temperature range of 100–1200 °C it was possible to distinguish three temperature zones of physicochemical properties changing, that was discussed above for alumina monoliths.

In the temperature range of 100–700 °C the phase composition and pore volume (∼0.41 to 0.44 cm^3/g) of the titania monoliths do not change. As a result, this range of

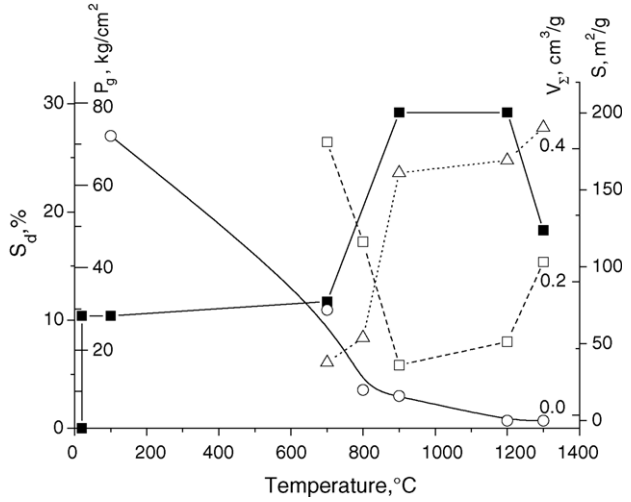

Fig. 6. Changes in the surface area, S, m^2/g (○); pore volume, V_Σ, cm^3/g (□); shrinkage, S_d, % (■); and mechanical strength, P_g, kg/cm^2 (△) of the titania monolith depending on calcination temperature.

calcination temperature has a minor effect on the geometrical dimensions of the samples (Fig. 6). The decrease of the specific surface area from 185 to 72 m^2/g (Fig. 6) observed after the temperature increase from 100 to 700 °C is due to sintering of small pores and growth of anatase particles. According to the XRD data, their average size grows from 70 to 300 Å (Table 3).

At 900 °C a sharp decrease of the total pore volume (from 0.41 to 0.08 cm^3/g) and surface area (from 72 to 16 m^2/g), as well as significant growth of the monolith strength (from 17 to 63 kg/cm^2) are observed (Fig. 6). The change of the sample texture is primarily caused by continuous sintering of small pores, which is indicated by an increase of the predominating pore radius from 160 to 400 Å and anatase particle size to 400–500 Å (Table 3). The change of the pore structure is also connected with beginning of the anatase phase transformation to rutile that ends at temperatures about 1050 °C (Table 3). A significant decrease of the pore volume leads to a sharp decrease of the sample geometrical dimensions down to 28–30% (Fig. 6).

At the temperature range of 1000–1200 °C the textural characteristics, geometrical dimensions and phase composition (rutile) of titania monoliths remain constant (Fig. 6).

A calcination temperature increase from 1200 to 1300 °C leads to an increase of the total pore volume (to 0.23 cm^3/g), predominating pore radii (to 2.7 μm) and, surprisingly, also increases geometrical dimension of titania samples and their mechanical strength (Fig. 6). Taking into account that the anatase to rutile phase transformation ends at 1050–1100 °C resulting in the formation of large rutile particles (~1000 Å) characterized by low surface area (~5 m^2/g), the textural changes of titania monolith are likely to be caused by decomposition of the Ca-montmorillonite binder. The montmorillonite melting temperature is about 1100 °C [13], and Ca or Mg silicates are the main products of its decomposition during high-temperature calcination. Apparently, the pore volume increase and the surface area decrease are caused by montmorillonite foaming during its decomposition with formation of a rigid glazed skeleton. The above supposition is in a good agreement with the XRD (Table 3) and SEM data.

3.3. Aluminosilicate honeycomb monoliths

The ^{1}H NMR technique is unacceptable for study of aluminosilicate monolith because the high concentrations of paramagnetic Fe^{3+} (~1.6 wt.%) ions lead to a strong diminution of the water spin relaxation time T_1 and T_2. In this case, we investigated the main physicochemical properties observed for aluminosilicate monoliths and on the basis of comparison with data for titania, we concluded that the texture formation regularities for these two substrates are similar. The calcination temperature increase of aluminosilicate monoliths from 700 to 900 °C is accompanied by a surface area decrease (from 37 to 0.4 m^2/g, Fig. 7) and a mechanical strength growth (from 22 to 39 kg/cm^3, Fig. 7). The pore volume of aluminosilicate monoliths does not practically change when the calcination temperature is increased from 700 to 1100 °C (Fig. 7), whereas the predominating pore radii grow from 300 to 1.5 μm (Table 4). A significant change in the geometrical dimensions of aluminosilicate monoliths about 8.5% along the sample diameter and length is observed at the dry-curing stage (Fig. 7). Practically no changes in the sizes of the studied monoliths (from 8.5 to ~10%) are observed after the following increase of the calcination temperature to 900–1100 °C (Fig. 7). Changes in the sample porosity are also insignificant (from 22 to 26%, Table 4).

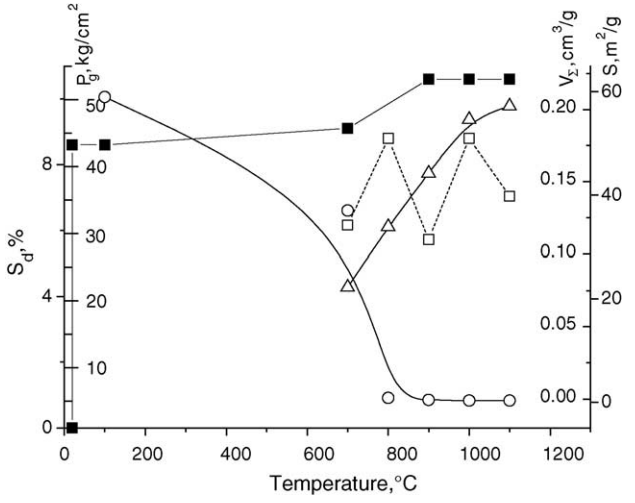

Fig. 7. Changes in the surface area, S, m^2/g (○); pore volume, V_Σ, cm^3/g (□); shrinkage, S_d, % (■); and mechanical strength, P_g, kg/cm^2 (△) of the aluminosilicate monolith depending on calcination temperature.

4. Conclusions

The main regularities of formation of honeycomb monoliths (alumina, titania and aluminosilicates) texture have been revealed using ^{1}H NMR imaging, SEM, XRD, adsorption technique, and others. The texture changes may be tentatively subdivided into several temperature regions.

At the temperature range of 20–100 °C, i.e. during dry-curing and drying of the samples, changes of the texture of the samples are related to removal of capillary water from the pore space of the material. Then the interaction of the hydroxyl groups of the binder (aluminum hydroxide sol or montmorillonite) with solid particles of the oxide material (γ-Al_2O_3, anatase, clay, etc.) leads to the strong bonds formation, which results in contraction of the structure. The contraction degree depends on the nature of the binder and is high for montmorillonite.

At the low-temperature calcination region (100–700 °C) changes in the texture of honeycomb monoliths take place due to sintering of small pores and consolidation of the oxide material particles, whereas no phase transformations are observed. The total pore volume does not practically change at this temperature range. Consequently, the geometrical dimensions of the sample are not changed. The upper limit of this temperature range is different for alumina, titania and aluminosilicate monoliths and corresponds to the phase transformation temperature.

At the high-temperature calcination region (above 900 °C) textural changes are related to phase transformations of the oxide component and the binder. Significant changes in volume and radius of pores accompanied by substantial changes of dimensions are observed in this temperature region.

Acknowledgements

This work was supported by INCO—COPERNICUS contract no ICA2-CT-1999-10028, INTAS-00413, NWO-RFBR 047.015.012.

References

[1] R.M. Heck, R.J. Farrauto, Catalytic air pollution control, in: Commercial Technology, VNR, New York, 1995 , p. 206.
[2] A. Cybulski, J.A. Moulijn, Catal. Rev. -Sci. Eng. 36 (2) (1994) 179.
[3] F. Kapteijn, J. Heiszwolf, T. Nijhuis, J. Monlijn, Cat. Tech. 3 (1) (1999) 24.
[4] Z.R. Ismagilov, Abstract Book of Internet. Seminar "Monolith honeycomb supports and catalysts", St. Petersburg, Russia, 1995, p. 9.
[5] I. Lachman, J. Williams, Catal. Today 14 (1992) 317.
[6] V.Yu. Prokofyev, A.P. Ilyin, Yu.G. Shirokov, E.N. Yurchenko, Zhurnal Prikladnoi Khimii 68 (1995) 781.
[7] I.V. Koptyug, V.B. Fenelonov, L.Yu. Khitrina, R.Z. Sagdeev, V.N. Parmon, J. Phys. Chem. B 102 (1998) 3090.
[8] S. Davies, M.Z. Kalam, K.J. Packer, F.O. Zelaya, J. Appl. Phys. 67 (1990) 3171.
[9] P.J. Prado, B.J. Balcom, M. Jama, J. Magn. Reson. 137 (1999) 59.
[10] V.A. Dzisko, A.P. Karnaukhov, D.V. Tarasova, Physicochemical Bases for Synthesis of Oxide Catalysts, Nauka, Novosibirsk, 1978, p. 278 (in Russian).
[11] Z.R. Ismagilov, R.A. Shkrabina, N.A. Koryabkina, Catal. Today 47 (1999) 51.
[12] D.I. Trimm, A. Stanislaus, Appl. Catal. 21 (1986) 215.
[13] V.I. Perelman (Ed.), Chemist's Short Dictionary, Khimiya, Moscow, 1964, p. 280 (in Russian).